BOLETÍN GEOLÓGICO Y MINERO 136 (1)
enero-marzo 2025, 010
ISSN-L: 0366-0176, eISSN: 2253-6167
https://doi.org/10.21701/bolgeomin/136.1/010

Boletín
Geológico y
Minero

RESEARCH ARTICLE

New Ar-Ar geochronology of the Catanda carbonatitic magmatism (Angola) and implications on its origin

Nueva geocronología Ar-Ar del magmatismo carbonatítico de Catanda (Angola) e implicaciones sobre su origen

Darío Chinchilla-Benavides[1*], Enrique Merino-Martínez[1], Manuela Chamizo-Borreguero[1], Pablo Valverde-Vaquero[1], Aratz Beranoaguirre[2], Janet Gabites[3], José Manuel[4]

[1]Centro Nacional Instituto Geológico y Minero de España, IGME (CSIC), Ríos Rosas 23, 28003 Madrid.
[2]Institute of Applied Geosciences (AGW), Karlsruhe Institute of Technology (KIT), Adenauerring 20b,76131 Karlsruhe, Germany.
[3]Pacific Center for Isotopic and Geochemical Research, The University of British Columbia, Vancouver, Canadá.
[4]Instituto Geológico de Angola, IGEO. Centralidade do Kilamba, Rua Nr, Luanda (Angola)

Corresponding author: d.chinchilla@igme.es (Darío Chinchilla Benavides)

Key point:

New Ar-Ar dates obtained in PLANAGEO project suggest different magmatic and metasomatic events recorded in the carbonatitic melts.

Older whole-rock Ar-Ar ages may suggest different metasomatic events in the lithospheric mantle below the complex.

Ar-Ar ages in phlogopite and those reported in mineral separates suggest a Pliocene to Pleistocene carbonatitic magmatism.

ABSTRACT

The Catanda Complex is one of the few examples of extrusive carbonatitic volcanoes in the world, and the only one known in Angola. It occurs along the Lucapa corridor that runs SW-NE across Angola. Kimberlitic, alkaline (mostly syenitic to ijolitic terms) and carbonatitic intrusions mark this corridor out that runs SW-NE across Angola. This magmatism was previously related to the Mesozoic continental rifting and the opening of the South Atlantic Ocean. However, recent geochronology from the carbonatitic volcanics of the Catanda Complex indicates that these volcanic rocks are much younger (0.56-0.78 Ma), and related to the Pleistocene reactivation of Mesozoic structures coeval with the formation of the East African rift. Newly acquired Ar^{39}-Ar^{40} geochronology during the PLANAGEO project illustrates the complexities of dating these carbonatitic melts. The whole-rock Ar-Ar spectra shows a U-shape pattern indicative of excess-Ar with a series of well-defined steps at 471 ± 28 Ma and 210 ± 6 Ma, confirmed by the intercepts of their separate Ar-isochrons. The geological significance of these dates is questionable, but this Ar-spectra could indicate the presence of older Ar reservoirs. A phlogopite separate from the same sample does provide a reliable spectra with an Ar-Ar plateau age of 3.01 ± 0.53 Ma and a concordant Ar-isochron age of 2.83 ± 0.66 Ma. This age is slightly older than the previously reported ages suggesting the existence of several carbonatitic magmatic pulses in the Catanda area during the Pliocene-Pleistocene.

Keywords: Alkaline-carbonatitic magmatism; Ar-Ar geochronology; Extrusive carbonatites; Catanda; Angola.

Article History:
Received: 21/02/2024
Accepted: 05/03/2025
Published: 22/08/2025

Puntos clave:

Las nuevas dataciones Ar-Ar (PLANAGEO) sugieren distintos eventos magmáticos y metasomáticos registrados en los fundidos carbonatíticos.

Las edades Ar-Ar en roca total más antiguas podrían sugerir diferentes eventos metasomáticos en el manto litosférico bajo el complejo.

RESUMEN

El Complejo de Catanda es uno de los pocos ejemplos de volcanes carbonatíticos extrusivos del mundo y el único conocido en Angola. Se encuentra en el corredor de Lucapa, el cual atraviesa Angola en dirección SW-NE. Intrusiones kimberlíticas, alcalinas (principalmente sieníticas a ijolíticas) y carbonatíticas caracterizan este corredor. Este magmatismo se relacionó anteriormente con el *rifting* Mesozoico y la apertura del océano Atlántico Sur. Sin embargo, la geocronología reciente de las rocas carbonatíticas del Complejo de Catanda indica que estas son más jóvenes (0.56-0.78 Ma), y están relacionadas con la reactivación pleistocena de estructuras mesozoicas, coetáneas con la formación del *rift* de África Oriental. La geocronología Ar^{39}-Ar^{40} obtenida durante el proyecto PLANAGEO, de una colada carbonatítica, ilustra las complejidades de la datación de estos fundidos carbonatíticos. El espectro Ar-Ar de roca total muestra una forma de U indicativa de exceso de Ar con escalones bien definidos a 471 ± 28 Ma y 210 ± 6 Ma, confirmados por las edades de intersección en las isócronas de Ar. El significado geológico de estas edades es cuestionable, pero este espectro de Ar podría indicar la presencia

Las edades Ar-Ar en flogopita y las reportadas en separados minerales sugieren un magmatismo carbonatítico desde el Plioceno al Pleistoceno.

de reservorios de Ar más antiguos. Un separado de flogopita de la misma muestra proporciona un espectro fiable con una edad Ar-Ar plateau de 3,01 ± 0,53 Ma y una edad isocrona concordante de 2.83 ± 0.66 Ma. Esta edad es ligeramente más antigua que las edades anteriormente publicadas, sugiriendo la existencia de varios pulsos magmáticos carbonatíticos el área de Catanda durante el Plioceno-Pleistoceno.

Palabras clave: Geocronología Ar-Ar; Magmatismo alcalino-carbonatítico; Carbonatitas volcánicas; Catanda; Angola.

Historial del artículo:
Recibido: 21/02/2024
Aceptado: 05/03/2025
Publicado: 22/08/2025

Citation / Cómo citar este artículo: Chinchilla-Benavides, D., Merino-Martínez, E., Chamizo-Borreguero, M., Valverde-Vaquero, P., Beranoaguirre, A., Gabites, J., Manuel, J. (2025). New Ar-Ar geochronology of the Catanda carbonatitic magmatism (Angola) and implications on its origin. Boletín Geológico y Minero, 136(1), 010. https://doi.org/10.21701/bolgeomin/136.1/010

1. Introduction

The Catanda Carbonatite Complex (CCC) represents one of the few examples of extrusive carbonatites in the world, constituting a unique volcanic carbonatite complex in west Angola (Woolley & Church, 2005; Bambi, 2015; Campeny, 2016). This carbonatitic volcanic system has a complex structure associated to explosive and effusive volcanic activity. It is made up of eight main eruptive centres, whose carbonatite magmas have a high content of F, Nb and Rare Earth Elements (Bambi, 2015; Campeny, 2016; Campeny *et al.,* 2014, 2015). For that reason and with the aim of enhancing the geological knowledge of SW Angola, the Catanda volcanic complex has been an intriguing subject of study during the PLANAGEO Project (National Geology Plan of Angola).

Catanda is one of the three main regions in Angola that contains carbonatitic complexes (Issa Filho *et al.*, 1991). These carbonatite-rich areas are the central (Monte Verde, Bailundo, Coola, Longonjo, Tchivira-Bonga), southwest (Virulundo, Lupongola), and central-west (Catanda) regions. These areas are usually associated with the alkaline-carbonatitic magmatism that occurred during Mesozoic times in SW Angola. This magmatism is distributed along a series of tectonic alignments that were active at least during the Upper Jurassic and Lower Cretaceous (155 Ma, 138-130 Ma; Lapido-Loureiro, 1973; Cahen *et al.,* 1984; Allsopp & Hargraves, 1985; Issa Filho *et al.,* 1991; Coltorti *et al.,* 1993; Alberti *et al.,* 1999; Comin-Chiaramonti *et al.,* 2005, 2007). These large-scale tectonic structures control the distensive Lucapa structure, the Alkaline-carbonatitic Diagonal Trans-Angola Province (Woolley, 1987; Lapido-Loureiro, 1967, 1968, 1973, 1995), and the Volcanic Belt of Angola (Machado, 1959), which are associated with the destabilisation and crustal break-up of Pangaea promoted by the opening of the South Atlantic Ocean (Guardado *et al.,* 1989; Brownfield & Charpentier, 2006, Torsvik *et al.,* 2009; Bryant *et al.,* 2012).

The petrographic and geochemical features of the CCC have been widely studied in the works of Melgarejo *et al.* (2012), Bambi (2015), Campeny *et al*. (2015, 2017), Campeny (2016) and Giuliani *et al.* (2017). Nevertheless, the existing geochronological data regarding the Catanda magmatism may be contradictory. For example, the phonolite dikes found near the CCC presumably associated with this carbonatitic magmatism, were dated at 92 ± 7 Ma by whole-rock K-Ar geochronology (Silva & Pereira, 1973; Torquato & Amaral, 1973; in Torquato, 1977), indicating association with the opening of the Atlantic Ocean. However, recent ^{39}Ar-^{40}Ar and (U-Th-Sm)/He mineral dating of the Catanda lavas (Campeny, 2016; Giuliani *et al.,* 2017), which yield extrusion ages ranging from 0.78 to 0.56 Ma (Pleistocene), suggests a relationship with the reactivated ancient NE-SW extensional structures in the context of the crustal fracturing and alkaline- carbonatitic magmatism currently occurring in the East African Rift. Nevertheless, Ar-Ar ages from phlogopite separates recently obtained in PLANAGEO, together with additional whole-rock Ar-Ar dating of the same carbonatitic sample, provide a new insight on the geological history of the Catanda region in central west Angola. In any case, the variability of the radiometric values encourages discussion for future geological and geochronological work in the area.

2. Geological setting

The CCC is located in the Kwanza Sul province (Angola), approximately 60 km southeast of the town of Sumbe (Fig. 1). This complex comprises a cluster of relatively eroded volcanic cones, covering an area of 50 km^2, composed of carbonatitic lavas and pyroclastic materials unconformably deposited over a Paleoproterozoic igneous and metasedimentary basement (Fig. 1). The CCC preserves the morphology of a volcanic building, although intense alteration and erosion have caused the development of eluvial-alluvial deposits on the slopes of this building. In the Chiva lagoon area, to the east of the main volcanic building, there are carbonatite dikes associated with the complex (Campeny *et al.*, 2017). In the vicinity of this volcanic complex, active hot springs have also been described associated with a NNW-SSE fault system that emanates CO_2-rich waters, resulting in the formation of thick travertine deposits on top of the Palaeoproterozoic basement (Bambi, 2015).

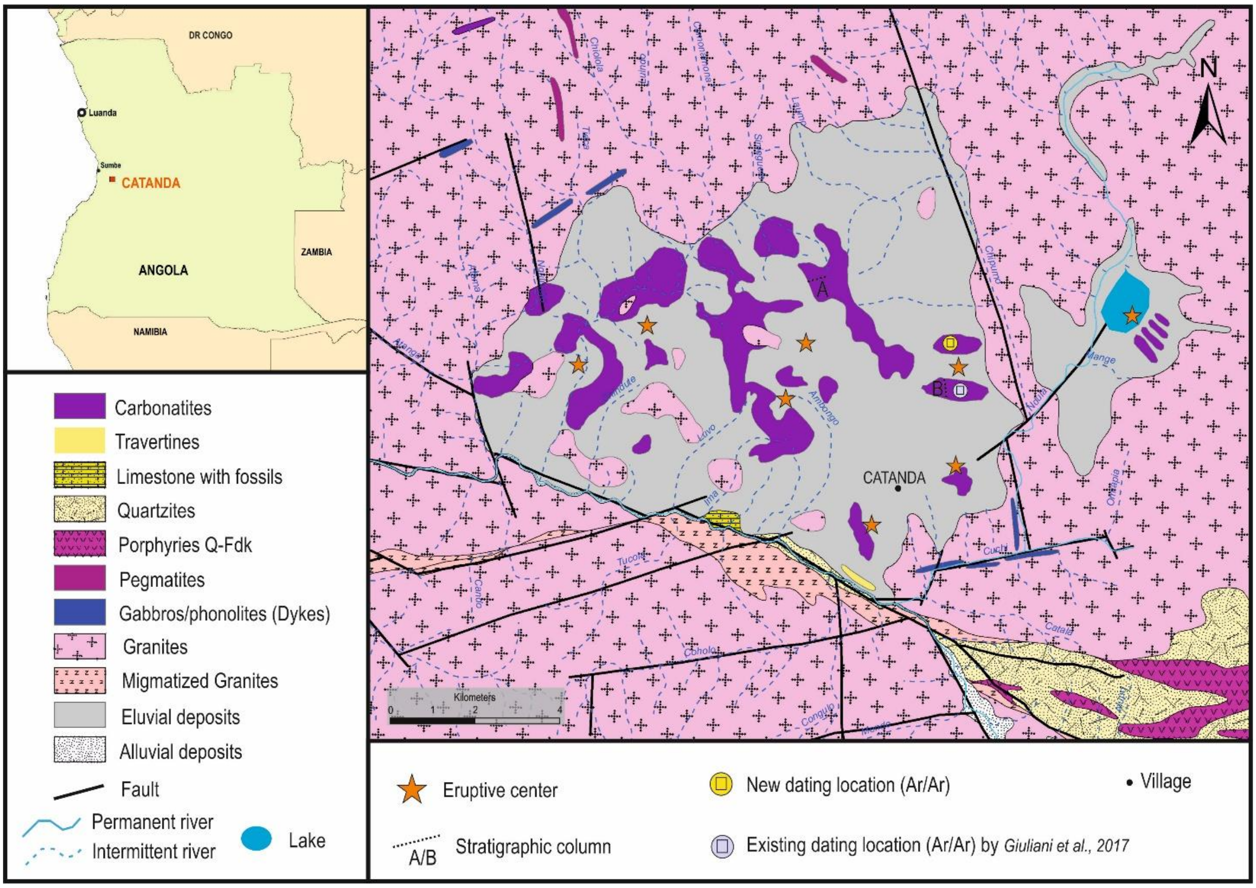

Figure 1. Geographic location and geological map of the Catanda area. It is also indicated the location of the stratigraphic sections A and B performed during the PLANAGEO project.

Figura 1. Localización geográfica y mapa geológico del área de Catanda. También se indica la ubicación de las columnas estratigráficas A y B realizadas durante el proyecto PLANAGEO.

The basement and country rock of the CCC comprise slightly foliated, porphyritic and medium-grained Palaeoproterozoic granitoids affected by a complex system of brittle, occasionally ductile, fracturing with WNW-ESE, NNW-SSE and ENE-WSW directions. In some of these sectors, the granite intrusions display medium- to high strain deformational textures, showing cataclastic to mylonitic textures, and more sparsely preserved migmatitic structures. Metasedimentary rocks and quartz-feldspar porphyries occur within a WNW-trending high-strain deformational corridor. The granitoid basement is intruded by a set of NNW-SSE and ENE-WSW trending microgabbros and phonolite dikes. These latter alkaline dikes provided an age of 92 ± 7 Ma by whole-rock K-Ar (Torquato & Amaral, 1973). Given the spatial association with these alkaline dykes, the CCC was interpreted as Cretaceous in age.

3. The Catanda Carbonatite Complex: field and petrographic features.

The Catanda Carbonatite Complex (CCC) stands out as a topographic height with an elevation of < 200 m over the surrounding countryside (Fig. 2). Carbonatitic pyroclastites and lavas of calciocarbonatite, silicocarbonatite and natrocarbonatite composition form a composite volcanic structure, as a result of different extrusive and effusive events (Fig. 3; Bambi, 2015; Campeny, 2016), defining anticlinal structures associated with the flanks of the volcanic building. Campeny *et al.* (2017) cite the presence of explosive and effusive maar-type structures, located in the Chiva lagoon, related to the carbonatitic magmatism of Catanda. The petrography of these rocks is described in detail in the works of Melgarejo *et al.* (2012), Bambi (2015), Campeny *et al.* (2014, 2015, 2017), Campeny (2016) and Giuliani *et al.* (2017).

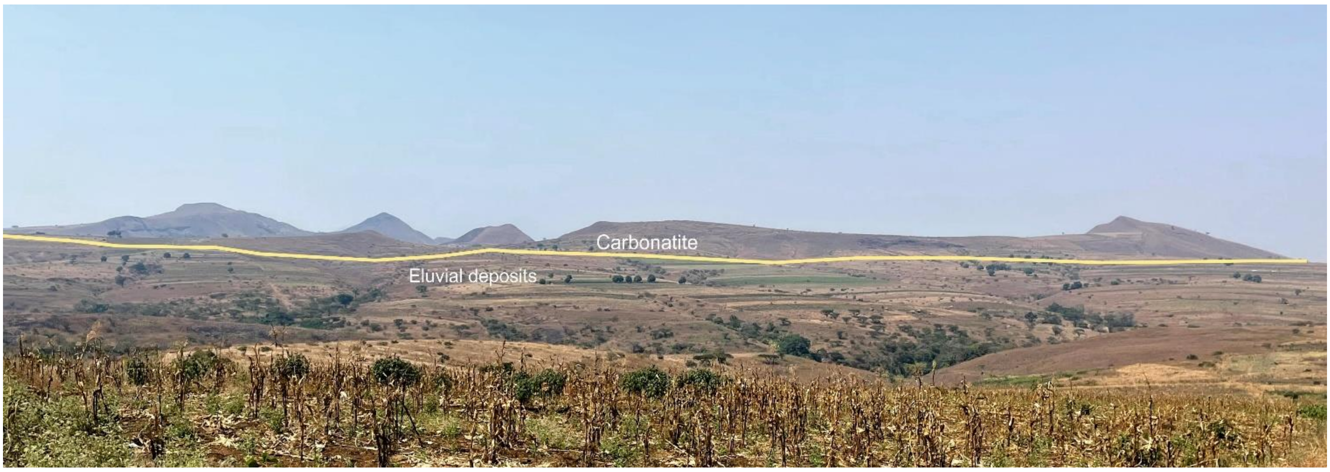

Figure 2. Panoramic view of the Catanda Carbonatitic Complex (CCC) from the NE. The shape of the volcanic edifice is partially preserved and the carbonatite outcrops can be seen at the top of the image, whereas the eluvial deposits covering the entire area appear at the bottom of the image.

Figura 2. Vista panorámica del Complejo Carbonatítico de Catanda desde el NE. Se conserva parcialmente la forma del edificio volcánico y se pueden ver los afloramientos de carbonatitas en la parte superior de la imagen, y los depósitos eluviales que cubren toda el área en la parte inferior de la imagen.

The pyroclastic deposits of the CCC seem to be linked to explosive episodes related to the high volatile content of the carbonatitic magmas. These deposits consist of fine- to medium-grained pyroclastites with cinerite levels, the latter typically deposited at the top of the sequence (figs. 3A, E and 4). They usually show pale, fiery to slightly yellowish colours (figs. 3A, B). The tuff levels and pyroclastites may present carbonate cement, which increases their competence and resistance to weathering. They usually present parallel, grain-decreasing, lamination and planar or cross stratification (figs. 3C, D). These deposits are composed of calcite, apatite, pyroxene, quartz and amphibole crystals (Bambi, 2016). The pyroclastic levels usually include heterolithic fragments of foliated granitoids and porphyritic granites, and more sparsely, gabbros and serpentinised ultramafic rocks, associated with host-rock brecciation during the carbonatite magma ascent, and extrusion of volcanic products (Fig. 3E). Some of these fragments show signs of metasomatism related to the circulation of hydrothermal fluids and/or volatile enrichment occurring after the extrusion of the carbonatitic pulses.

Effusive carbonatite lava flows tend to occur at high structural levels within the volcanic edifice. The dark grey to greenish colours of these materials, together with their high competence, make them more visible in the most prominent heights of the sequence (figs. 3F, G). They have an inequigranular porphyritic holocrystalline texture, with subhedral to anhedral apatite, calcite and phlogopite phenocrysts, and olivine, magnetite and pyroxene xenocrysts, the latter showing reaction rims (figs. 3H, J).

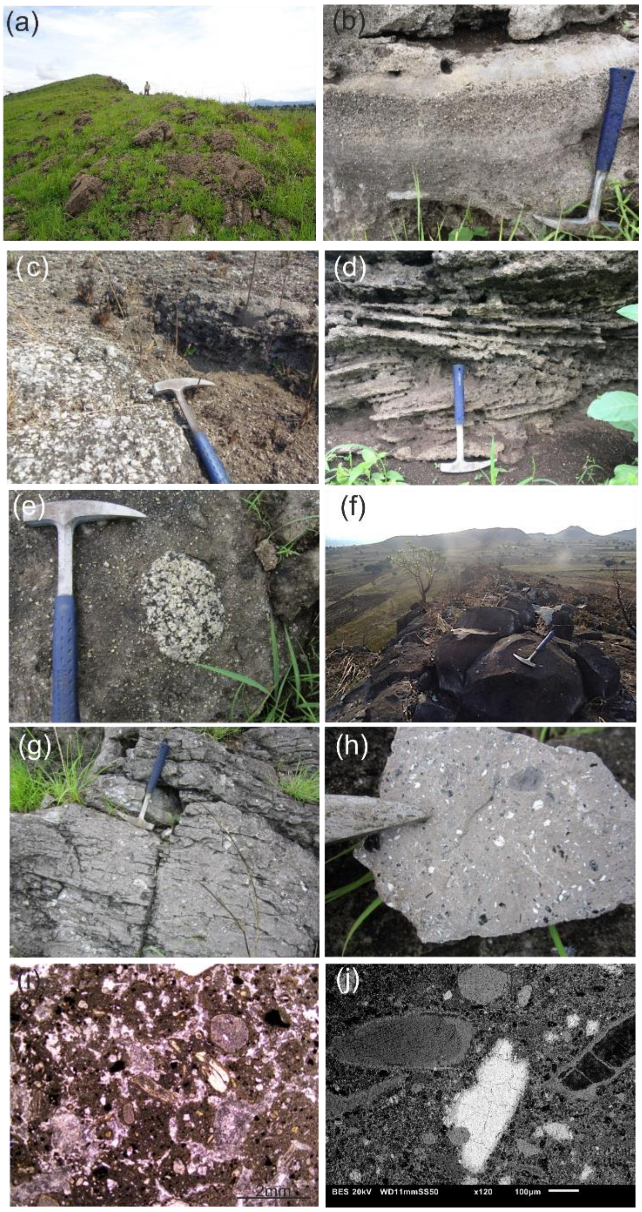

Figure 3. Mesoscopic and microscopic features of the Catanda volcanic rocks. a) Fine- to medium-grained pyroclastic deposits, forming a steep slope of the volcanic edifice. b) Alternation of fine- to medium-grained pyroclastites and cinerites, showing greyish to slightly yellowish light colours. c) Carbonatite pyroclastites deposited unconformably over the Palaeoproterozoic granitic basement. d) Cross-bedded fine- to medium-grained pyroclastites. e) Detail of a fragment of a porphyritic granite included in the pyroclastite deposits. f) Competent levels of carbonatite lavas, showing dark colours and high relief. g) Carbonatite lava flow corresponding to the upper half of stratigraphic column B. h) Detail of the carbonatite lava flow, showing apatite and calcite phenocrysts and mafic xenocrystic (olivine, pyroxene), with reaction halos at the edges. i) Microphotograph of the carbonatite lava flow, showing phlogopite, hornblende, clinopyroxene and olivine phenocrysts in a matrix composed of carbonates, opaque minerals and zeolites. j) Scanning electron microscope (SEM) microphotograph of a pyroclastic flow, showing abundant phenocrysts within a fine-grained matrix. Reaction halos in grain edges are observed in the phenocrysts.

Figura 3. Características mesoscópicas y microscópicas de los materiales volcánicos de Catanda. a) Materiales piroclásticos de grano fino a medio, que forman una pendiente pronunciada del edificio volcánico. b) Alternancia de piroclastitas y cineritas de grano fino a medio, con colores claros, grises a ligeramente amarillentos. c) Piroclastitas carbonatíticas depositadas en discordancia sobre las unidades del basamento granítico Paleoproterozoico. d) Piroclastitas de grano fino a medio con estratificación cruzada. e) Detalle de un fragmento de granito porfídico (roca encajante) incluido en los depósitos piroclásticos. f) Niveles competentes de lavas carbonatíticas, de tonalidades oscuras y elevado relieve. g) Colada carbonatítica correspondiente a la mitad superior de la columna B (Fig. 4. h) Detalle de la colada carbonatítica, mostrando fenocristales de apatito, calcita y xenocristales de minerales máficos (olivino, piroxeno), con halos de reacción en los bordes. i) Lámina delgada de la colada de lava carbonatítica, mostrando fenocristales de flogopita, hornblenda, clinopiroxeno y olivino en una matriz compuesta por carbonatos, minerales opacos y zeolitas. j) Microfotografía con microscopio electrónico de barrido (SEM) de una muestra piroclástica, donde se pueden observar abundantes fenocristales dentro de una matriz de grano fino. Se observan bordes de reacción en los fenocristales.

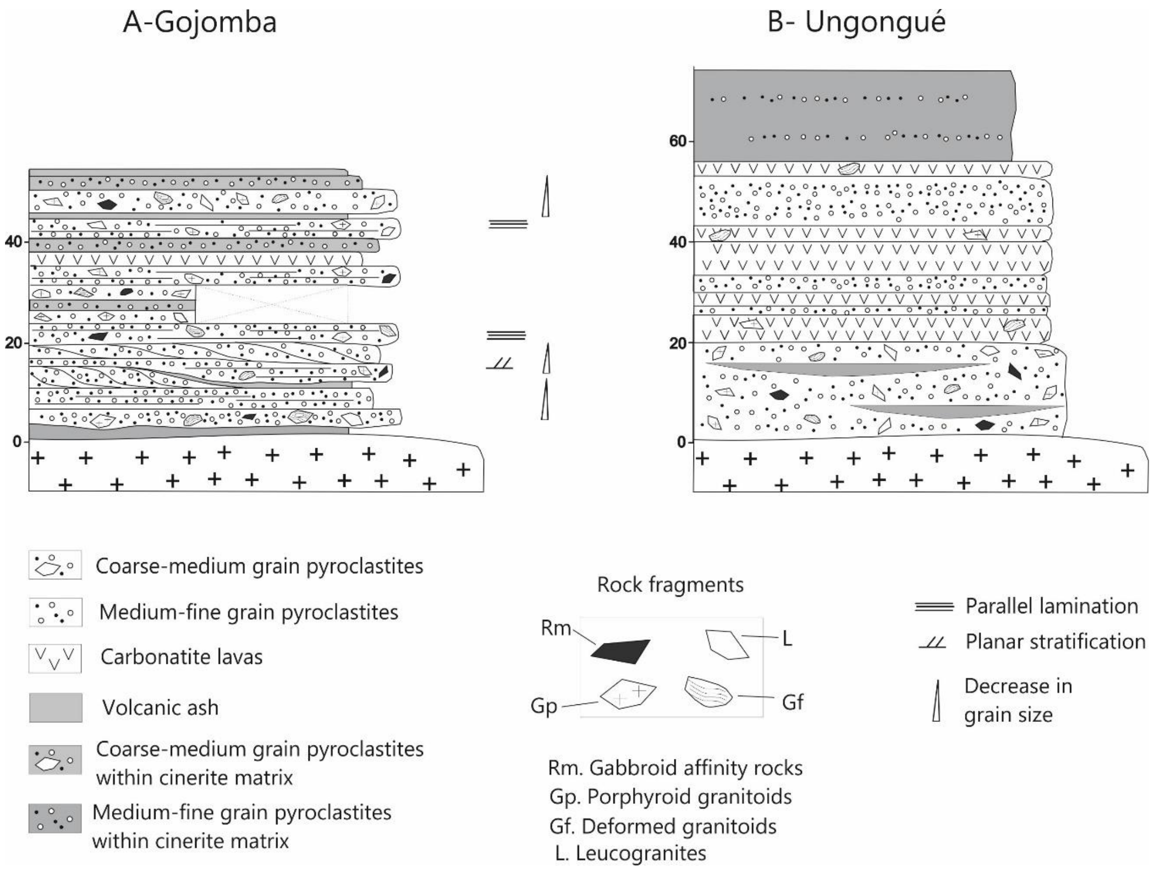

Figure 4. Stratigraphic columns of the Catanda Carbonatite Complex (CCC). Column A – Gonjomba is located on the NW of the area whereas the B-column is located on the SE of the complex. See location on Figure 1.

Figura 4. Columnas estratigráficas del Complejo Carbonatítico de Catanda. La columna A – Gonjomba está ubicada en el NO del área, mientras que la columna B está ubicada en el SE del complejo. Ver localización en la Figura 1.

The matrix forms a micro- to cryptocrystalline carbonate-rich mesostasis with brownish to violet colours, together with larger crystals of olivine, apatite, clinopyroxene, opaque minerals, and zeolites (Fig. 3H). Bambi (2015) and Campeny (2016) mentioned the presence of pyrochlore, fluorite, fluorapatite, spinel, baddeleyite and barite.

During PLANAGEO field work, two stratigraphic columns were made (Fig. 4; see location in Fig. 1). The column A-Gonjomba was studied in the NW area of the carbonatitic complex, with a total thickness of 58 meters. This section is dominated by pyroclastites rather than lava flows. The lower part (30 m) of the column consists of lenticular pyroclastic bodies with variable thickness and a lateral continuity of up to 18 m (Fig. 4A). These pyroclastite layers show a tendency to decrease in grain size towards the top, displaying planar cross-bedding and parallel lamination (Fig. 3D). The upper part of the section (28 m) is formed by pyroclastites of variable granulometry and laminated cinerites of massive appearance (Fig. 3B), interbedded with an approximately 5 m thick pyroclastic flow level with a large lateral continuity.

The second column (B-Ungongué) was constructed on the southern slope of a volcanic eruptive centre located in the eastern part of the complex, reaching a total thickness of almost 70 m. This section contains a higher concentration of pyroclastic materials compared to column A, covering almost 55 m of the section. The pyroclastite levels are heterometric and have an overall massive appearance (Fig. 4B). The presence of heterolithic fragments in the pyroclastic materials of the surrounding basement (gabbros, foliated granites and porphyritic granites) is constant along the two columns (Fig. 3E). The upper half of this section is dominated by massive carbonatite lava flows (figs. 3F, H). The sample dated in this study (UTEMC33U015I; UTM coordinates: (X) 441538 (Y) 8708575) was taken from this carbonatitic level.

4. Ar-Ar methodology

Sample preparation for Ar-Ar dating, including rock crushing and mineral separation (phlogopite in this case), was performed at the IGME laboratories in Tres Cantos (Madrid, Spain) and sent to the Pacific Center for Isotopic and Geochemical Research (PCIGR), University of British Columbia (Vancouver, Canada).

Samples were crushed and sieved to obtain fragments ranging in the size from 0.1 to 0.5 mm. A hand-magnet was passed over the samples to remove magnetic minerals and metallic crusher fragments/spall. The samples were rinsed in dilute nitric acid, washed in deionized water and then air-dried at room temperature. Mineral separates were hand-picked, wrapped in aluminium foil and stacked in an irradiation capsule with similar-aged samples and neutron flux monitors (Fish Canyon Tuff sanidine, 28.02 Ma; Renne *et al.,* 1998). The samples were irradiated at the McMaster Nuclear Reactor in Hamilton, Ontario, for 56 MWH, with a neutron flux of 3x1016 neutrons/cm^2. Analyses (n=54) of 18 neutron flux monitor positions produced errors of <0.5% in the J value. The mineral separates were step-heated at incrementally higher powers in the defocused beam of a 10W CO_2 laser (New Wave Research MIR10) until fused, at the Noble Gas Laboratory of the PCIGR facilities from the University of British Columbia. The gas evolved from each step was analysed with a VG5400 mass spectrometer equipped with an ion-counting electron multiplier. All measurements were corrected for total system blank, mass spectrometer sensitivity, mass discrimination, radioactive decay during and after irradiation, as well as interfering Ar from atmospheric contamination and the irradiation of Ca, Cl and K. Isotope production ratios were (^{40}Ar/^{39}Ar)K=0.0302, (^{37}Ar/^{39}Ar)Ca=1416.4306, (^{36}Ar/^{39}Ar)Ca=0.3952, Ca/K=1.83(^{37}ArCa/^{39}ArK). The plateau and correlation ages were calculated using Isoplot 3.09 software (Ludwig, 2003). Errors are quoted at the 2σ (95% confidence) level and are propagated from all sources except mass spectrometer sensitivity and age of the flux monitor.

5. Ar-Ar geochronological results

A carbonatite sample from a lava flow from an eruptive centre located in the eastern part of the CCC was selected for Ar–Ar isotopic analyses (sample UTEMC33U015I; Fig. 3H). Ar-Ar dating was performed on whole-rock and phlogopite separates of the same sample (figs. 5, 6). The whole-rock Ar-Ar spectra shows a "U" shape pattern of gas steps with different apparent ages (Fig. 5A). The first two initial heating steps display an average age of 1483 ± 67 Ma, due to the low ^{39}Ar (4.42-3.51 %) and radiogenic ^{40}Ar content (15.95-12.34%; Table 1), while the next two steps and the final one yield an average age of 471 ± 28 Ma. The remaining three continuous steps with 61% of the Ar released provide an Ar-Ar plateau age of 203 ± 19 Ma (MSWD = 0.028, probability = 0.97; Fig. 5A). The normal isochron age of the whole data reveals an inaccurate age of 170 ± 78 Ma (MSWD = 10.5; Fig. 5B). After pooling the concordant ^{40}Ar*/^{39}Ar results and discriminating the two age spectra, the corresponding inverse isochrons yield Ar-Ar ages of 461 ± 63 Ma for the oldest data (Fig. 5C), and 203 ± 49 Ma for the youngest steps (Fig. 5D), which are within the error of the Ar-Ar plateau ages.

The phlogopite separate provides an Ar-Ar plateau age of 3.01 ± 0.53 Ma (MSWD = 0.39, probability = 0.91, including 98.9% of ^{39}Ar; Fig. 6A). The two first steps were discarded for age calculations, due to their low ^{39}Ar (0.24 % and 0.81 %) and erratic radiogenic ^{40}Ar values (-237.9 % and -310.09 %) (Table 2). However, the remaining data showed a consistent average age throughout all heating stages, within error, supporting the confidence of the Ar-Ar plateau age obtained. In fact, the produced inverse isochron from the concordant Ar-Ar age data provides a similar age (i.e., 2.83 ± 0.66 Ma; Fig. 6B) to that obtained by the Ar-Ar plateau age, reinforcing the consistency of the age data.

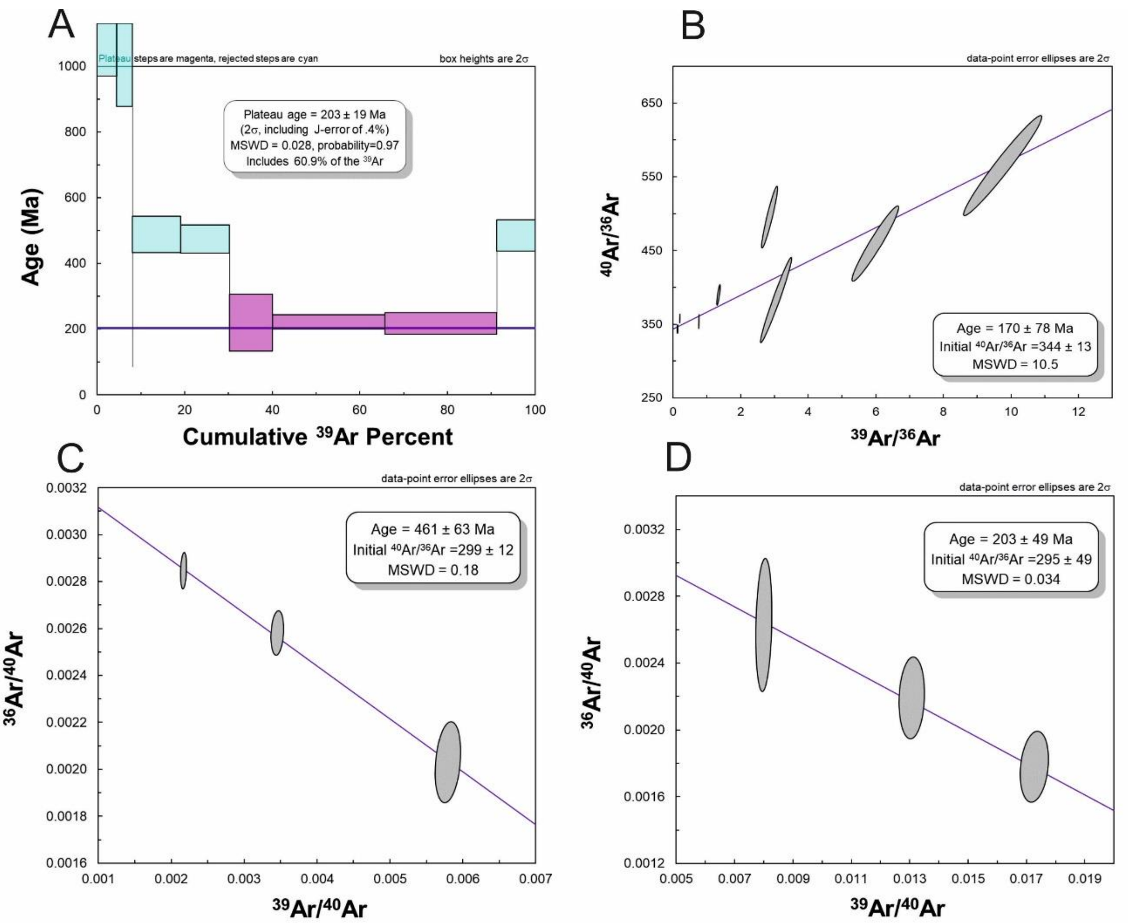

Figure 5. A) Whole-rock Ar/Ar plateau age obtained for the Catanda carbonatite lava flow (sample UTEMC33U015I) (203 ± 19 Ma); B) Whole-rock, normal isochron of the whole data, reporting an Ar-Ar age of 170 ± 78 Ma. C) Inverse isochron of the old concordant age data, giving an Ar-Ar age of 461 ± 63 Ma. D) Inverse isochron of the youg concordant data, showing an age of 203 ± 49 Ma.

Figura 5. A) Edad de plateau Ar/Ar en roca total de una colada carbonatítica de Catanda (muestra UTEMC33U015I). Magmatismo carbonatítico de Catanda (203 ± 19 Ma); B) Edad de isocrona Ar-Ar obtenida a partir de todos los datos de edades, aportando una edad de 170 ± 78 Ma. C) Isocrona inversa de los datos concordantes antiguos, obteniéndose una edad Ar-Ar de 461 ± 63 Ma. D) Isocrona inversa de los datos concordantes jóvenes, mostrando una edad de 203 ± 49 Ma.

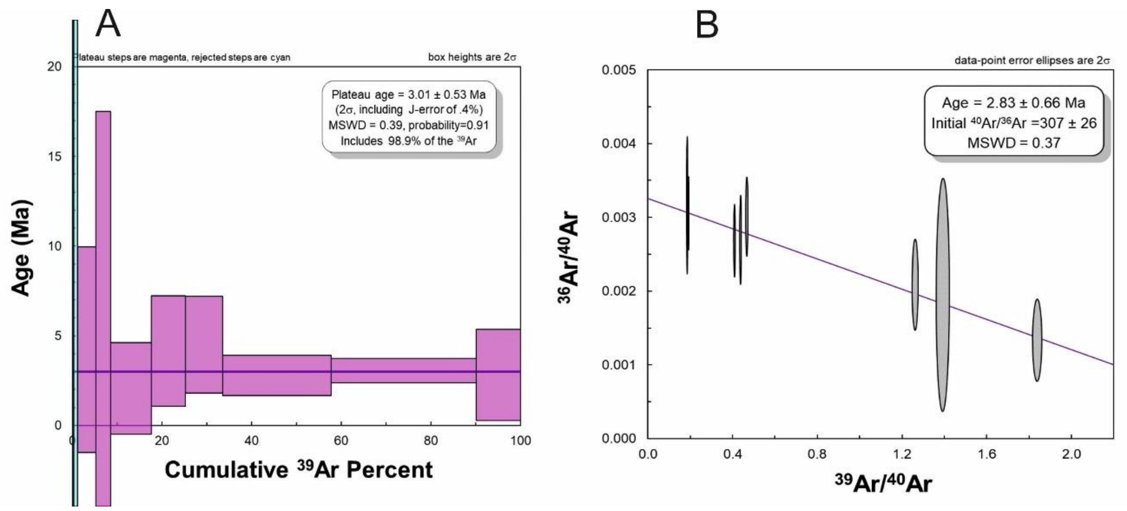

Figure 6. A) Ar/Ar Plateau age from phlogopite phenocrysts of the Catanda lava flow (UTEMC33U015I) (3.01 ± 0.53 Ma), B) Inverse isochron obtained from the concordant Ar-Ar age data, giving an age of 2.83 ± 0.66 Ma.

Figura 6. A) Edad de plateau Ar/Ar en separados de flogopita de la misma colada de Catanda (UTEMC33U015I) (3.01 ± 0.53 Ma), B) Isocrona inversa obtenida a partir de los datos de edad Ar-Ar concordantes, aportando una edad de 2.83 ± 0.66 Ma.

Laser	*Isotope Ratios*														
Power(%)	$^{40}Ar/^{39}Ar$	2σ	$^{36}Ar/^{39}Ar$	2σ	$^{39}Ar/^{40}Ar$	2σ	$^{36}Ar/^{40}Ar$	2σ	*Rho*	*K/Ca*	*%*^{40}Ar *rad*	*f* ^{39}Ar	$^{40}Ar^{*}/^{39}ArK$	*Age*	2σ
2,30	1721,39	35,15	4,86	0,12	0,0006	0,00001	0,0028	0,00004	0,053	0,01	15,95	4,42	281,893	1457,80	± 79,57
2,60	2305,16	135,51	6,80	0,41	0,0004	0,00003	0,0029	0,00004	0,026	0,00	12,34	3,51	307,483	1546,83	± 127,34
3,00	433,71	6,23	1,26	0,03	0,0022	0,00003	0,0028	0,00006	0,223	0,01	14,99	11,14	69,072	477,93	± 56,00
3,40	257,89	3,91	0,72	0,02	0,0035	0,00007	0,0026	0,00008	0,193	0,00	23,02	11,16	66,716	463,53	± 43,95
3,80	118,32	3,32	0,34	0,04	0,0080	0,00023	0,0026	0,00033	0,183	0,01	21,61	9,80	27,004	201,95	± 88,25
4,50	56,56	1,31	0,11	0,01	0,0172	0,00040	0,0018	0,00018	0,213	0,02	47,17	25,72	27,353	204,42	± 22,93
5,20	73,59	1,92	0,18	0,01	0,0131	0,00035	0,0022	0,00020	0,108	0,01	34,82	25,43	26,670	199,59	± 33,66
6,00	160,77	3,81	0,36	0,02	0,0058	0,00014	0,0020	0,00014	0,248	0,01	39,59	8,83	68,469	474,26	± 48,50

J = 0.00431950 ± 0.00000864 Volume ^{39}ArK = 0,078 x E-13 cm^3 NPT

Integrated Date = 343,76 ± 15,09 Ma

Plateau age = 203 ± 19 Ma (2σ, including J-error of .4%) MSWD = 0.028, probability=0.97 Includes 60.9% of the ^{39}Ar steps 5 through 7

Inverse isochron (correlation age) results: Model 1 Solution (± 95%-conf.) on 3 points

Age = 461 ± 63 Ma Initial $^{40}Ar/^{36}Ar$ =299 ± 12 MSWD = 0.18 Probability = 0.67

Inverse isochron (correlation age) results: Model 1 Solution (± 95%-conf.) on 3 points

Age = 203 ± 49 Ma Initial $^{40}Ar/^{36}Ar$ =295 ± 49 MSWD = 0.034 Probability = 0.85

Table 1. Results of whole rock Ar-Ar studies on sample: UTEMC33U015I.

Tabla 1. Resultados de los estudios Ar-Ar en roca total en la muestra: UTEMC33U015I.

Laser	*Isotope Ratios*														
Power(%)	$^{40}Ar/^{39}Ar$	2σ	$^{36}Ar/^{39}Ar$	2σ	$^{39}Ar/^{40}Ar$	2σ	$^{36}Ar/^{40}Ar$	2σ	*Rho*	*K/Ca*	*%*^{40}Ar *rad*	*f* ^{39}Ar	$^{40}Ar^{*}/^{39}ArK$	*Age*	2σ
2,40	56,61	2,33	0,64	0,14	0,02	0,0007	0,0113	0,0025	0,052	0,12	-237,95	0,24	135,153	-2052,03	± 1173,29
2,80	35,11	0,28	0,48	0,07	0,03	0,0002	0,0137	0,0021	0,009	0,30	-310,09	0,81	109,027	-1436,38	± 438,71
3,20	5,11	0,04	0,0157	0,0021	0,20	0,0015	0,0030	0,0004	0,035	2,59	8,98	4,13	0,459	4,19	± 5,75
3,50	5,30	0,05	0,0168	0,0041	0,19	0,0019	0,0032	0,0008	0,032	1,78	5,65	3,25	0,299	2,73	± 11,08
3,90	2,13	0,02	0,0064	0,0009	0,47	0,0037	0,0030	0,0004	0,033	4,50	10,47	9,13	0,222	2,03	± 2,56
4,30	2,27	0,02	0,0061	0,0011	0,44	0,0042	0,0027	0,0005	0,038	6,06	19,90	7,63	0,452	4,12	± 3,07
4,80	2,43	0,02	0,0065	0,0010	0,41	0,0031	0,0027	0,0004	0,031	8,08	20,17	8,27	0,490	4,47	± 2,69
6,20	0,79	0,01	0,0022	0,0004	1,26	0,0113	0,0021	0,0005	0,021	0,37	38,24	24,26	0,303	2,76	± 1,10
7,20	0,54	0,00	0,0012	0,0002	1,84	0,0169	0,0013	0,0005	0,019	0,38	60,97	32,39	0,332	3,02	± 0,68
8,20	0,72	0,01	0,0017	0,0009	1,40	0,0254	0,0019	0,0013	0,025	0,67	42,55	9,91	0,305	2,78	± 2,54

J = 0.00498690 ± 0.00000997 Volume ^{39}ArK = 1,326 x E-13 cm^3 NPT

Integrated Date = 3,01 ± 0,53 Ma

Plateau age = 3.01 ± 0.53 Ma (2σ, including J-error of .4%) MSWD = 0.39, probability=0.91 Includes 98.9% of the ^{39}Ar steps 3 through 10

Inverse isochron (correlation age) results: Model 1 Solution (±95%-conf.) on 8 points

Age = 2.83 ± 0.66 Ma Initial $^{40}Ar/^{36}Ar$ =307 ± 26 MSWD = 0.37 Probability = 0.9

Table 2. Results of Ar-Ar studies on phlogopite separates from the sample: UTEMC33U015I.

Tabla 2. Resultados de los estudios Ar-Ar en separados de flogopita de la muestra: UTEMC33U015I

6. Discussion

The Catanda volcanic complex was commonly considered to be formed during Cretaceous times (e.g., Silva & Pereira, 1971; Issa Filho *et al*., 1991; Alberti *et al.,* 1999), according to the whole-rock K-Ar crystallisation age of 92 ± 7 Ma reported for the tinguaite dikes located southeast of Catanda (Torquato & Amaral, 1973). The U-Pb geochronological works performed in kimberlites from the Catoca region, to the east of Catanda, provided an eruption age of 117.9 ± 0.7 Ma (Robles-Cruz *et al*., 2012). Other works provide crystallisation ages of some alkaline-carbonatitic massifs in Angola comprised between 130 and 155 Ma, using Rb-Sr isochron or Ar-Ar plateau ages (Cahen *et al.,* 1984; Allsopp & Hargraves, 1985; Merino-Martínez, 2022; Merino-Martínez *et al.,* 2025), suggesting a clear relationship between this magmatism and the breakup of Gondwana and the opening of the South Atlantic Ocean. Nevertheless, the works of Campeny (2016) and Giuliani *et al.* (2017) attributed an extrusion age for the Catanda carbonatite lavas between 0.56 and 0.78 Ma based on ^{39}Ar-^{40}Ar in phlogopite and (U-Th-Sm)/He in apatite isotopic dating. These authors considered these ages to be associated with the reactivation of Cretaceous structures, such as the Lucapa corridor, during the middle Pleistocene.

The Ar-Ar data obtained in the PLANAGEO project, presented in this study, together with the previously reported Ar-Ar data (Campeny, 2016; Giuliani *et al.,* 2017) suggest that this magmatism took place between 3 and 0.5 Ma. Excess argon is responsible for the U-shaped Ar-Ar spectra displayed by the whole-rock sample. This feature is commonly associated with low potassium rocks or the presence of melt or fluid inclusions, which would release far more argon during stepwise heating, producing anomalously old ages (e.g., Kelley, 2002, and references therein). Also, it can be attributed to the presence of excess Ar in the mantle source of these magmas (e.g., Coltice & Ricard, 2002). Thus, although the whole rock Ar-Ar plateau ages displayed in the Catanda carbonatite lava flow could reflect distinct incorporation mechanisms for the excess argon (Fig. 5A), they may be also indicative of old magmatic events and/or mantle metasomatic imprints recorded by the carbonatitic magmas, these latter without connection to any precise tectono-thermal event identified at the surface of the region so far.

The younger Ar-Ar plateau ages of 203 ± 19 are similar to the whole-rock K-Ar age of 222 ± 16 Ma reported in basaltic lava flows found in the Kwanza Basin (Torquato & Amaral, 1973). It is worth noting that within the PLANAGEO project other recent Ar-Ar dating in basaltic samples south to the Sumbe area also reveal an Ar-Ar plateau age of 210 ± 6 Ma (Merino-Martínez *et al.,* 2021), which closely aligns with the results obtained in the Catanda samples. These ages are also alike to those reported in dolerite dikes from the Espinhaço Region and Santos Basin of Brazil (220-193 Ma; Dossini *et al.,* 1995; Guedes *et al*., 2005) and closely resemble those documented in the Central Atlantic Magmatic Province (204-192 Ma; Svensen *et al.,* 2017; Oliveira *et al.*, 2023). This would suggest that: i) the Catanda magmatism was related to the pre-Karoo magmatism recorded in the Central Atlantic Magmatic Province, and may correspond to the first basaltic pulses occurred during the early stages of crustal break-up of the Pangaea supercontinent during the Triassic-Jurassic transition (Svensen *et al.,* 2017); or ii) that high-temperature xenolith minerals and/or inclusions were incorporated in the carbonatite materials, revealing a late-Triassic metasomatism event in the lithospheric mantle beneath the Catanda volcanics, similar to that suggested for other Cenozoic alkaline volcanics (e.g., Villaseca *et al.*, 2018).

Possible evidence for mantle metasomatic events could be also recorded in this Ar spectra. The initial whole-rock Ar ages constrained between 1547 and 1458 Ma (average age of 1483 ± 67 Ma) would probably attest for erratic measurements due to excess Ar (Fig. 5A; Table 1). Nevertheless, similar ages are documented in SW Angola and NW Namibia, related to the emplacement of distinct igneous intrusions and MT to HT metamorphic events registered in the Epupa Complex during the late-Palaeoproterozoic and Early-Mesoproterozoic (1534-1447 Ma Brandt *et al.,* 2003; Seth *et al.,* 2003, 2005).

In addition, some steps of the whole-rock Ar-Ar dating performed in the carbonatitic lavas of Catanda also display an average age of 471 ± 28 Ma. This age matches the ages recorded in the post-orogenic stages of the Pan-African/Brasiliano orogeny (Heilbron *et al.,* 2008; Bento dos Santos *et al.,* 2010, 2015). It is interesting to note that other similar ages have been determined within the PLANAGEO Project (i.e., 509-475 Ma; Chamizo & Buzzi, 2021; Lopes *et al.,* 2021; Merino-Martínez, 2022) in distinct gneissic rocks from the Angolan coastal region and in dolerite dikes from SW Angola. Torquato & Amaral (1973) also reported equivalent K-Ar ages ranging from 508 ± 59 to 490 ± 8 Ma in granite and gneissic rocks to the west of Catanda. In fact, these ages are described in the coastal Angolan counterparts, the Ribeira Belt/Mantiqueira Province in SE Brazil and northern Uruguay, related to the cooling ages of long-term magmatism (540–490 Ma; Bento dos Santos *et al.,* 2010, 2015) or in the Cabo Frio tectonic domain, associated to the latest deformational events of the Brasiliano orogeny (505–490 Ma; Schmitt *et al.,* 2004, 2008).

On the contrary, the accurate Ar-Ar plateau age obtained from the phlogopite suggests an extrusion age for the carbonatitic lava flow of 3.01 ± 0.53 Ma (Fig. 6A). This age is older than the phlogopite Ar inverse isochron and U-Th-Sm/He apatite ages of 0.8-0.5 Ma obtained by Campeny (2016) and Giuliani *et al.* (2017) for other carbonatitic lavas of the CCC. Hence, the ages recorded in the CCC lava flows would suggest that distinct episodes of carbonatitic volcanism occurred during the Pliocene and Pleistocene in the Catanda region.

However, the Pliocene-Pleistocene age for the complex needs to be taken with caution, as Bambi (2015) and Campeny *et al*. (2014, 2015) described diverse alteration textures in the Catanda lavas, including the phlogopite crystals, as well as evidence of geochemical and isotopic ($\delta^{13}C$-$\delta^{18}O$) mobility related to hydrothermal processes. This hydrothermalism could account for the disturbance of the age spectra and spread of the Ar phlogopite and U-Th-Sm/He apatite ages reported for the Catanda carbonatites. In addition, it should be noted that several meteoric alteration and erosion phenomena occurred from the Cretaceous to the Pleistocene (Pereira, 1977), and a significant crustal uplift, which formed the so-called Chela Escarpment, was described between Miocene and Pliocene times (Jackson *et al.,* 2005; Guiraud *et al.,* 2010). Thus, further geochronological and isotopic work is required to better constrain the timing of the carbonatitic volcanism and associated hydrothermalism in the CCC and its connection with the Cenozoic volcanism in central Africa (Giuliani *et al.,* 2017).

7. Conclusions

The newly acquired Ar-Ar dates within the PLANAGEO project prompt further discussion on the geochronology of the carbonatitic lavas found in the Catanda volcanic complex of central west Angola. The Ar-Ar data determined in whole-rock and phlogopite mineral separates from a carbonatitic lava provide significantly different ages. The whole-rock analysis provides a U-shape Ar-Ar spectra characteristic of excess Ar, with a plateau age of 210 ± 6 Ma. The geological significance of this age is arguable, but it could suggest that a late-Triassic metasomatic event could have been recorded in the lithospheric mantle beneath the CCC, related to the initial stages of magmatism during the opening of the South Atlantic Ocean. Initial whole-rock Ar steps with an average age of 1483 ± 67 Ma and an inverse Ar isochron age of 471 ± 28 Ma, although probably derived from excess Ar, could also attest for older thermal and/or metasomatic events registered in the lithospheric mantle or the presence of Mesoproterozoic and/or Palaeozoic sources beneath the Catanda region. A separate set of phlogopite crystals have provided an Ar-Ar plateau age of 3.01 ± 0.53 Ma, that is alike to the obtained concordant inverse isochron Ar age of 2.83 ± 0.66 Ma. This newly acquired Ar data, together with the previously reported ages in mineral separates (0.78-0.56 Ma in phlogopite and apatite), suggests a Pliocene-Pleistocene extrusion age for the Catanda Carbonatite Complex.

Acknowledgments

This work is a result of the National Geological Plan of Angola (PLANAGEO). This project was supported by the Government of the Republic of Angola and implemented by the Geological Survey of Angola (IGEO), under the oversight of the Angolan Ministry of Mineral Resources, Oil and Gas (MIREMPET). We would like to express our gratitude for the invaluable assistance provided by the local staff, who facilitated the challenging conditions during our fieldwork and geological sampling. We also highly appreciate the precious contribution of the staff of Impulso Industrial Alternativo to this project.

Authorship contribution statement

Darío Chinchilla-Benavides: Writing - Original Draft, Investigation, Conceptualization, Methodology, Data Curation, Visualization, Supervision, Writing - Review & Editing.
Enrique Merino-Martínez: Writing - Original Draft, Investigation, Methodology, Data Curation, Investigation, Project administration, Formal analysis, Supervision.
Manuela Chamizo-Borreguero: Investigation, Supervision, Review & Editing.
Pablo Valverde-Vaquero: Investigation, Data Curation, Formal analysis, Writing - Review & Editing.
Aratz Beranoaguirre: Data Curation, Investigation, Formal analysis.
Janet Gabites: Data Curation, Investigation, Visualization.
José Manuel: Supervision, Project administration, Funding acquisition.

References

Alberti, A., Castorina, F., Censi, P., Comin-chiaramonti, P., & Gomes, C.B. (1999). Geochemical characteristics of Cretaceous carbonatites from Angola. Journal África Earth Sciences, 29(4), 735-759.

Allsopp, H.L., & Hargraves, R.B. (1985). Rb-Sr ages and palaeomagnetic data for some Angolan alkaline intrusives. Transactions Geological Society South Africa, 88, 295-299.

Bambi, A.C.J.M. (2015). Metalogenia de las carbonatitas en dominios plutónicos, subvolcánicos y volcánicos: Tchivira, Bonga y Catanda, Angola. Tese de doutorado. Universitat de Barcelona. 705 pp.

Bambi, A. C. J. M. (2016). Metalogenia de las carbonatitas en dominios plutónicos, subvolcánicos y volcánicos: Tchivira, Bonga y Catanda, Angola.

Bento dos Santos, T. M., Munhá, J. M., Tassinari, C. C., Fonseca, P. E., & Neto, C. D. (2010). Thermochronology of central Ribeira Fold Belt, SE Brazil: Petrological and geochronological evidence for long-term high temperature maintenance during Western Gondwana amalgamation. Precambrian Research, 180 (3-4), 285-298.

Bento dos Santos, T. M. B., Tassinari, C. C., & Fonseca, P. E. (2015). Diachronic collision, slab break-off and long-term high thermal flux in the Brasiliano–Pan-African orogeny: Implications for the geodynamic evolution of the Mantiqueira Province. Precambrian Research, 260, 1-22.

Brandt, S. (2003). Metamorphic evolution of ultrahigh-temperature granulite facies and upper amphibolite facies rocks of the Epupa Complex, NW Namibia. Unpublished PhD Thesis, University of Würzburg, Germany, 289 p.

Brownfield, M. E., & Charpentier, R. R. (2006). Geology and total petroleum systems of the west-central coastal province (7203), West Africa (No. 2207-B). US Geological Survey.

Bryant, I., Herbst, N., Dailly, P., Dribus, J. R., Fainstein, R., Harvey, N., & Tapponnier, P. (2012). Basin to basin: Plate tectonics in exploration. Oilfield Review, 24(3), 38-57.

Cahen, L., Snelling, N.J., Delhal, J., & Vail, J.R. (1984). The geochronology and evolution of África: London, Oxford University Press, 512 p.

Campeny, M. (2016). Caracterización del vulcanismo carbonatítico de Catanda (Angola). Tésis de Doutoramento, Universitat de Barcelona, 66 pp.

Campeny, M., Kamenetsky, V.S., Melgarejo, J.C., Mangas, J., Alfonso, P., Kamenetsky, M.B., Bambi, A.C.J.M., & Gonçalves, A.O. (2015). Carbonatitic lavas in Catanda (Kwanza Sul, Angola): Mineralogical and geochemical constraints on the parental melt. Lithos, 232, 1-11.

Campeny, M., Mangas, J., Melgarejo, J. C., Bambi, A., Alfonso, P., Gernon, T., & Manuel, J. (2014). The Catanda extrusive carbonatites (Kwanza Sul, Angola): an example of explosive carbonatitic volcanism. Bulletin of Volcanology, 76, 1-15.

Campeny, M., Melgarejo, J.C., Mangas, J., & Gonçalves, A.O. (2017). Recent carbonatitic magmatism in Angola: the dykes of the Chiva lagoon maar. Boletín de la Sociedad Geológica Mexicana, 209-220.

Chamizo, M., & Buzzi, J. (2021). Carta Geológica de Angola à escala 1:100.000, folha 250-251 (Benguela), e memória explicativa. UTE (IGME, LNEG, Impulso) - IGEO, Luanda, 156 pp.

Coltice, N., & Ticard, Y. (2002). On the origin of noble gases in mantle plumes. Phil. Trans.R.Soc. Lond. A, 360, 2633-2648.

Coltorti, M., Alberti, A., Beccaluva, L., Dos Santos, A.B., Mazzucchelli, M., Morais, E., Rivalenti, G., & Siena, F. (1993). The Tchivira Bonga alkaline-carbonatite complex (Angola): petrological study and comparison with some Brazilian analogues. Eur. J. Mineral., 5, 1001-1024.

Comin-Chiaramonti, P., Barros Gomes, C., Cundari, Al., Castorina, F., & Censi, P. (2007). A review of carbonatitic magmatism in the Paraná-Angola-Namibia (PAN) system. Periodico di Mineralogia, 76(2-3), 25-78.

Comin-Chiaramonti, P., Gomes, C. B., Marques, L. S., Censi, P., Ruberti, E., & Antonini, P. (2005). Carbonatites from southeastern Brazil: geochemistry, OC, Sr-Nd-Pb isotopes and relationships with the magmatism from the Paraná-Angola-Namibia Province. Mesozoic to Cenozoic alkaline magmatism in the Brazilian Platform. Edusp/Fapesp, São Paulo, 657-688.

Dossini, T.M., Dossini, I.A., Charvet, J., & Bonhomme, M.G. (1995). K-Ar chronology of a Mesozoic dike swarm from southern Espinhaço Region (SE Brazil). Journal of South American Earth Sciences, 8(1), 47-53.

Giuliani, A., Campeny, M., Kamenetsky, V. S., Afonso, J. C., Maas, R., Melgarejo, J. C., & Manuel, J. (2017). Southwestern Africa on the burner: Pleistocene carbonatite volcanism linked to deep mantle upwelling in Angola. Geology, 45(11), 971-974.

Guardado, L. R., Gamboa, L. A. P., & Lucchesi, C. F. (1989). Petroleum geology of the Campos Basin, Brazil, a model for a producing atlantic type basin: In: Edwards, J.D., and Santogrossi, P.A. (eds.), Divergent/Passive Margin Basins. American Association of Petroleum Geologists 48. https://doi.org/10.1306/M48508C1

Guedes, E., Heilbron, M., Vasconcelos, P.M., Valeriano, C.M., Horta de Almeida, J.C., Teixeira, W., & Thomaz Filho, A. (2005). K–Ar and $^{40}Ar/^{39}Ar$ ages of dikes emplaced in the onshore basement of the Santos Basin, Resende area, SE Brazil: implications for the south Atlantic opening and Tertiary reactivation. Journal of South American Earth Sciences, 18(3-4), 371-382.

Guiraud, M., Buta-Neto, A., & Quesne, D. (2010). Segmentation and differential post-rift uplift at the Angola margin as recorded by the transform-rifted Benguela and oblique-to-orthogonal-rifted Kwanza basins. Marine and Petroleum Geology, 27, 1040-1068.

Heilbron, M., Valeriano, C. D. M., Tassinari, C. C. G., Almeida, J., Tupinamba, M., Siga Jr, O., & Trouw, R. (2008). Correlation of Neoproterozoic terranes between the Ribeira Belt, SE Brazil and its African counterpart: comparative tectonic evolution and open questions. Geological Society, London, Special Publications, 294(1), 211-237.

Issa Filho, A., Dos Santos, A.B.R.M.D., Riffel, B.F., Lapido-Loureiro, F.E.V., & McReath, I. (1991). Aspects of the geology, petrology and chemistry of some Angolan carbonatites. J. Geochem. Explor., 40, 205-226.

Jackson, M. P. A., Hudec, M. R., & Hegarty, K. A. (2005). The great West African Tertiary coastal uplift: Fact or fiction? A perspective from the Angolan divergent margin. Tectonics, 24(6), TC6014, 24 pp.

Kelley, S. (2002). Excess argon in K–Ar and Ar–Ar geochronology. Chemical Geology, 188, 1-22.

Lapido-Loureiro, F.E.V. (1967). Nota prévia sobre as estruturas carbonatiticas de Angola. Bol. Inst. Invest. Cient., Angola, Luanda 4(2), 45-66.

Lapido-Loureiro, F.E.V. (1968). Sub-volcanic carbonatite structures of Angola. In: XXIII International Geological Congress. Praga, pp. 147-161.

Lapido-Loureiro, F.E. (1973). Carbonatitos de Angola. Memórias e Traballos. I.I.C.A., 11.

Lapido-Loureiro, F.E.V. (1995). A mega-província carbonatítica Brasil-Angola e os seus recursos minerais; geologia, petrografia, geoquímica, geologia económica. Universidade de Lisboa, PhD Thesis, 191 pp.

Lopes, R., Pereira, L. F., Caessa, P., & Correia, J. (2021). Carta Geológica de Angola à escala 1:250.000, folha Sul D-33/G (Equimina), e memória explicativa. UTE (IGME, LNEG, Impulso) - IGEO, Luanda, 296 pp.

Ludwig, K.R. (2003). Isoplot 3.00 A Geochronological Toolkit for Microsoft Excel. Berkeley Geochronology Center, Special Publication No. 4.

Machado, A. D. B. (1959). New Systematic and Biogeo-graphical Studies of Glossina. Publicacoes Culturais Com-panhia Diamantes de Angola, (46), 13-90.

Melgarejo, J. C., Costanzo, A., Bambi, A. C., Gonçalves, A. O., & Neto, A. B. (2012). Subsolidus processes as a key factor on the distribution of Nb species in plutonic carbonatites: The Tchivira case, Angola. Lithos, 152, 187-201.

Merino-Martínez, E. (2022). Carta Geológica de Angola à escala 1:100.000, folha 336 (Lubango), e memória explicativa. UTE (IGME, LNEG, Impulso) - IGEO, Luanda, 172 p.

Merino-Martínez, E., Chinchilla, D., and Chamizo, M. (2021). Carta Geológica de Angola à escala 1:250.000, folha Sul C-33/U (Ucu Seles, metade Sul), e memória explicativa. UTE (IGME, LNEG, Impulso) - IGEO, Luanda, 175 p.

Merino-Martínez, E., Valverde-Vaquero, P., Beranoaguirre, A., Galán, G., Gabites, J., & Manuel, J. (2025). Preliminary Ar-Ar geochronology of Cretaceous alkaline-carbonatitic to tholeiitic magmatism in the Quilengues area, SW Angola. Boletín Geológico y Minero, (136).

Oliveira, A.L., Schmitz, M.D., Wall, C.J., Crowley, J.L., Macêdo Filho, A.A., & Hollanda, M.H.B.M. (2023). New U–Pb geochronology for the Central Atlantic Magmatic Province, critical reevaluation of high-precision ages and their impact on the end-Triassic extinction event. Science Reports, 13, 5485. https://doi.org/10.1038/s41598-023-32534-3.

Pereira, E. (1977). Serra da Neve, Angola: nota sobre a geomorfologia da regiao e idade das aplanaçoes.(Serra da Neve, Angola: note sur la géomorphologie de la région et notes sur les aplanissements). Boletim da Sociedade geologica de Portugal Lisboa, 20(3), 277-282.

Renne, P.R., Swisher, C.C., III, Deino, A.L., Karner, D.B., Owens, T., & DePaolo, D.J. (1998). Intercalibration of standards, absolute ages and uncertainties in $^{40}Ar/^{39}Ar$ dating. Chemical Geology, 145, 117-152.

Robles-Cruz, S. E., Escayola, M., Jackson, S., Galí, S., Pervov, V., Watangua, M., & Melgarejo, J. C. (2012). U–Pb SHRIMP geochronology of zircon from the Catoca kimberlite, Angola: implications for diamond exploration. Chemical geology, 310, 137-147.

Silva, M.V.S., & Pereira, E. (1971). Notícia Explicativa da carta Nº 207 GUNGO, escala 1:100 000. Direcção Provincial dos Serviços de Geologia e Minas, Luanda.

Silva, M.V.S., & Pereira, E. (1973). Estrutura Vulcânico-Carbonatítica da Catanda (Angola). Boletim dos Serviços de Geologia e Minas, 24, 5-14.

Schmitt, R. S, Trouw, R. A., Van Schmus, W. R., & Pimentel, M. M. (2004). Late amalgamation in the central part of West Gondwana: new geochronological data and the characterization of a Cambrian collisional orogeny in the Ribeira Belt (SE Brazil). Precambrian Research, 133(1-2), 29-61.

Schmitt, R.S, Trouw, R. A. J., Medeiros, S. R., & Dantas, E. L. (2008). Age and geotectonic setting of Late Neoproterozoic juvenile mafic gneisses and associated paragneisses from the Ribeira belt (SE Brazil) based on geochemistry and Sm–Nd data—implications on Gondwana assembly. Gondwana Research, 13(4), 502-515.

Seth, B., Armstrong, R.A., Brandt, S., Villa, I.M., & Kramers, J.D. (2003). Mesoproterozoic U–Pb and Pb–Pb ages of granulites in NW Namibia: reconstructing a complete orogenic cycle. Precambrian Research, 126, 147-168. https://doi.org/10.1016/S0301-9268(03)00193-1

Seth, B., Armstrong, R.A., Büttner, A., & Villa, I.M. (2005). Time constraints for Mesoproterozoic upper amphibolite facies metamorphism in NW Namibia: a multi-isotopic approach. Earth and Planetary Science Letters, 230, 355-378. https://doi.org/10.1016/j.epsl.2004.11.022

Svensen, H.H., Torsvik, T.H., Callegaro, S., Augland, L., Heimdal, T.H., Jerram, D.A., Planke, S., & Pereira, E. (2017). Gondwana Large Igneous Provinces: plate reconstructions, volcanic basins and sill volumes. Em: Sensarma, S. e Strorey, B.C. (eds). Large Igenous Provinces from Gondwana and Adjacent Regions. Geological Society, Special Publications, 463.

Torquato, J.R., & Amaral, G. (1973). Idades K/Ar em rochas das regiões de Catanda e Vila do Almoster. Bol. Inst. Invest. Cient., Angola, Luanda, vol. 10, Pub. IICA 308.

Torquato, J. R. (1977). Geotectonica Outline of Angola. Cah. O.R.S.T.O.M., sér. Geól., vol. IX, nº 1/2, 15-34.

Torsvik, T. H., Rousse, S., Labails, C., & Smethurst, M. A. (2009). A new scheme for the opening of the South Atlantic Ocean and the dissection of an Aptian salt basin. Geophysical Journal International, 177(3), 1315-1333.

Villaseca, C., Belousova, E.A., Barford, D.N., & González-Jiménez, J.M. (2018). Dating metasomatic events in the lithospheric mantle beneath the Calatrava volcanic field (central Spain). Lithosphere, 11(2), 192-208.

Woolley, A. R. (1987). Alkaline rocks and carbonatites of the world. Part 3. The Geological Society of London. 372 p.

Woolley, A. R., & Church, A. A. (2005). Extrusive carbonatites: a brief review. Lithos, 85(1-4), 1-14.